Preparation and study of structural properties of zinc-doped barium stannate

C. DOROFTEI*, P. D. POPA[a], F. IACOMI
"Al. I. Cuza" University, Faculty of Physics, 11 Carol I Blvd, 7000506 Iasi, Romania.
[a]*Institute of Technical Physics, Bd. D. Mangeron 47, 700050 Iasi, Romania.*

In the present work, we report the results of the influence of the Zn ions that partly substitute the Ba ions in the barium stannate ($Ba_{1-x}Zn_xSnO_3$, where x = 0 - 0.5), on the structural properties. With the view to obtain a porous and finer structure, thus providing a high specific surface, these materials were obtained through the precursor method of combustion (co-precipitation in a colloidal environment, and combustion), followed by heat treatments. The phase composition and morphology were studied through XRD and SEM techniques. The pure sample, as well as that with the substitution $x < 0.1$, are single phased after 40 minutes sintering at 1000 ^oC. For substitutions with $x \geq 0.1$ secondary phases appear, but the structure becomes finer and the area of specific surface increases for x = 0.2, remaining then constant with the increasing doping with zinc ions up to x = 0.5. The sample with the substitution x = 0.2-0.5 is characterized by a very fine structure (~300 nm) and an effective porosity (21%). These materials obtained through this new method are quite promising for the realization of quality humidity or gas sensors.

(Received July 8, 2011; accepted April 11, 2012)

Keywords: Perovskites; Porous material; Ultrafine grained microstructure; SEM; XRD

1. Introduction

In the recent years, barium stannates received much attention do to their applications in humidity and gas sensors [1-3]. For a perovskite (ceramic) sensor, the microstructure and specific resistance of the sensor element are two key parameters on which its performance depends.

Generally, $BaSnO_3$ powders were prepared by solid-state reaction of $BaCO_3$ and SnO_3 at high temperature above 1300 ^oC. These powders contain impurities and are coarse grained [4]. The variation wet chemical syntheses, such as hydrothermal method [5], sol-gel method [4] and polymerized complex method [6,7] were recently reported for the preparation of the fine $BaSnO_3$ powders.

S. Upadhyay et al [8] reported the preparation of barium stannate doped nickel ions ($BaSn_{1-x}Ni_xO_3$ for x = 0-0.2) have been synthesized by solid state reaction method. There are few works focused on the utilization of zinc ions as dopants for the barium stannate.

In this work we meant to realize new materials with perovskite type structure (ABO_3) with big chances to be used in the realization of gas or humidity sensors. In the case of barium stannate, the preference of the substitute ions to the A and B sites in the perovskite structure can modify the structural and micro structural properties, namely the properties of sensitivity to humidity or to certain gases [9,10].

We chose the barium stannate for the following reasons:

- The barium stannate prepared through the precursor combustion method has a marked porosity;
- It has a fine granulation, as compared to that obtained through other classical preparation methods, which ensures a high specific surface;
- The Ba^{2+} ions ensure a high resistivity in dry condition.

Barium stannate is a cubic perovskite oxide compound which behaves as n-type semiconductor with a wide band gap of 3.4 eV and is stable at high temperature (up to 1000 ^oC) [11]. Various methods of synthesis of the barium stannate have been reported [7,12-15].

The present work reports the results of the influence of Zn^{2+} ions which partially substitute the Ba^{2+} ion in the barium stannate ($Ba_{1-x}Zn_xSnO_3$, where x = 0; 0.1; 0.2 and 0.5), on the structural properties. The Zn^{2+} ion was chosen as a substitute due to its ion radius very different from that of the Ba^{2+} ion which it replaces in the lattice to a small extent, up to x = 0.1 [16], while for bigger substitutions, the generation of secondary phases is expected, which improves the grain size and effective porosity. The method used to obtain these materials is the precursor method of combustion followed by heat treatments [17,18]. This method has some advantages because it improves the compositional homogeneity of the powders and, as a result, the microstructural homogeneity of the fired product - resulting perovskite powder is fine-grained and with porous structure [19].

2. Experimental

Zinc-doped barium stannates having the general formula $Ba_{1-x}Zn_xSnO_3$, where x=0-0.5 ($BaSnO_3$ (BZS-0), $Ba_{0.9}Zn_{0,1}SnO_3$ (BZS-1), $Ba_{0.8}Zn_{0,2}SnO_3$ (BZS-2) and

$Ba_{0.5}Zn_{0,5}SnO_3$ (BZS-3) were prepared by combustion method followed by heat treatments. Fig.1 shows the flow-diagram of the sample preparation process.

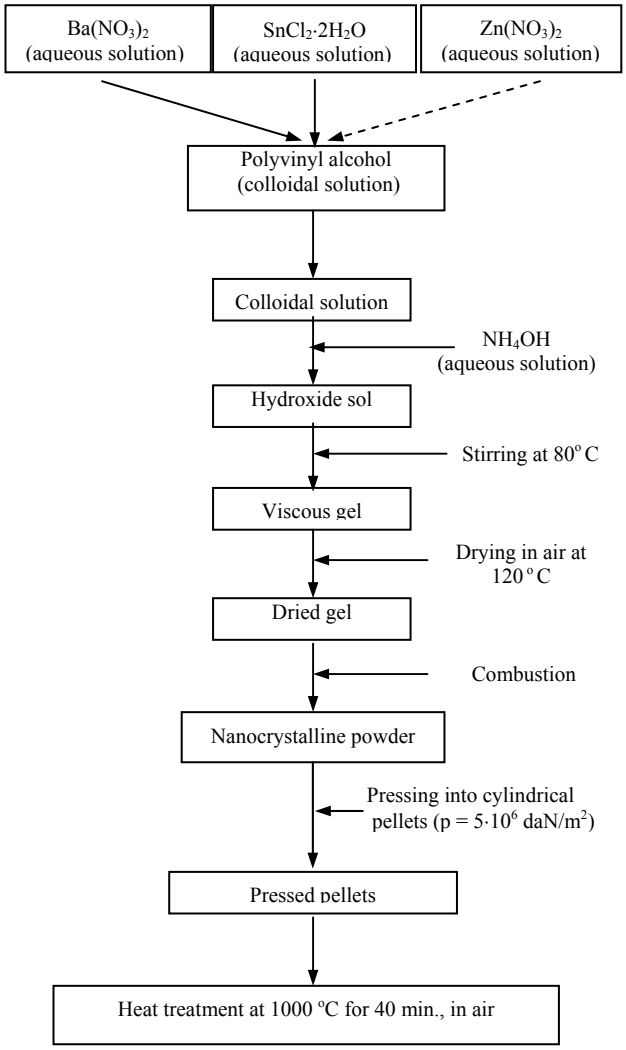

Fig. 1 Flow diagram for the fabrication process of $Ba_{1-x}Zn_xSnO_3$ (x = 0-0.5) fine powders by combustion method.

We used metal nitrates or chlorides as starting materials (starting from barium and zinc nitrates and stannous chloride as raw materials). Polyvinyl alcohol was added to make a colloidal solution. Molar ratio of metal to polyvinyl alcohol was 1:1. NH_4OH solution (25% concentration) was dropped to adjust the pH value at about 8. The combustion reaction converts the dried gel in a loose powder with nanogranular structure. The combustion obtained powders were heat treated for 6 hours at the temperature of 600 °C to finish the reaction and to make the carbon traces vanish. This procedure is more efficient than the conventional solid state reaction (physical mixture of oxides) for the preparation of ceramic powders, because it improves the compositional homogeneity of the powders and, as a result, the microstructural homogeneity of the fired product [19].

The reactions for $BaSnO_3$ can be schematized as follows:

$$Ba(NO_3)_2 + 2NH_4OH \rightarrow Ba(OH)_2 + 2NH_4NO_3 \quad (1)$$

$$SnCl_2 + 2NH_4OH \rightarrow Sn(OH)_2 + 2NH_4Cl\uparrow \quad (2)$$

$$C_2H_3OH + 5NH_4NO_3 \rightarrow 2CO_2\uparrow + 12H_2O\uparrow + 8N_2\uparrow + Q \quad (3)$$

$$Ba(OH)_2 + Sn(OH)_2 \rightarrow BaO + SnO + 2H_2O\uparrow \quad (4)$$

$$BaO + SnO + O \rightarrow BaSnO_3 \quad (5)$$

The obtained powders were mixed in a ball mill and biaxial pressed in a disc shape in a stainless steel die under a pressure of about 3×10^7 N/m^2. The pressed pellets (17 mm diameter, ~1.8 mm thickness) were sintered in air, at 1000 °C for 40 minutes and slowly cooled in the furnace. The weight and dimensions of the pellets were measured at room temperature, to determine the bulk density d and effective porosity p_{ef} (for open pores) using the Archimedes's principle [9,20].

The phase composition was identified by X-ray diffraction (XRD) using a diffractometer type DRON-3 and the CoK_α radiation (λ = 1.7889 Å). The values of the lattice parameter for all samples were obtained by the least square fitting of the XRD data using the "Crystalographica" software. The X-ray density, $d_x=M/Na^3$ [21] (where M is the molecular weight, N is Avogadro's number and a is the lattice constant) was used to evaluate the porosity $p=1-d/d_x$. The morphology was examined using a VEGA-TESCAN scanning electron microscope. The average grain size D_m was determined by the linear intercept technique from SEM micrograph on fracture surface [22]. The specific surface area was calculated from the equation $A_{sp}= s/v\cdot d=6/ D_m\cdot d$ [23, 24], where s and v are the particle surface and volume respectively, D_m is the average grain size, d is the bulk density and 6 is the shape factor. It is assumed that all the particles have the same size and shape.

3. Results and discussion

Fig. 2 (a and b) presents the X rays diffractographs of the BZS-0 ($BaSnO_3$) and BZS-3 ($Ba_{0.5}Zn_{0.5}SnO_3$) with the Miller indices which indicate the perovskite type structure, and with the secondary phases that appear. Only the BZS-0 (Fig. 2a) and BZS-1 samples were single-phased. The BZS-2 and BZS-3 samples (Fig. 2b) show several secondary phases. The presence of the secondary phases at the BZS-2 and BZS-3 samples suggests that the limit of Zn^{2+} ions solubility in the barium stannate lattice is $x \leq 0.1$. It is well known that the degree of host cation substitution by other foreign ions depends on the substitute cation radius [25]. The limitation of the zinc solubility in the barium stannate lattice is the result of the large difference between the ionic radius of Ba^{2+} (1.56Å) and

Zn^{2+} (0.88Å) ions respectively (Table 1). Upadhyay et al [16] also found out that the barium substitution in the barium stannate by ions with much smaller radius is generally restricted to x = 0.1.

Table 1. Characteristics of each ion in (BaZn)SnO_3 perovskite

Ion	Oxidation state	Electronegativity	Atomic weight (Kg)	Ionic radius (Å)
Ba	2+	1.0	0.137	1.56
Zn	2+	1.65	0.065	0.88
Sn	4+	1.7	0.118	0.69
O	-2	3.44	0.016	1.32

At the BZS-2 sample (x = 0.2), secondary phases like BaO, $Ba_3Sn_2O_7$, $ZnSnO_3$, SnO appear. At the BZS-3 (x = 0.5) sample (Fig. 2b), one can notice the presence of bigger amount of secondary phases: $ZnSnO_3$, $Ba_3Sn_2O_7$, Zn_2SnO_4, BaO, SnO_2, ZnO_2, etc.

The modification of the lattice parameter for the substituted samples can be accounted for by the presence of the Zn^{2+} ions on the substitution positions from the entire lattice of the barium stannate host. When a cation with the radius different from that of the host cation is introduced in a perovskite-type lattice, the difference between the host atoms and the substitutes creates a distortion in the perovskite-type lattice, which can affect the size of the elementary cell [8, 16]. The lattice constants for a high doping level, like in the case of BZS-2 and BZS-3 samples have very close values, which suggests that secondary phases with zinc in excess were formed, and the determined values for the lattice parameters are those of the crystalline core which contains a small amount of zinc.

The X-ray density is found to decrease with the increase of dopant concentration. This might be due to the replacement of heavier Ba-ions (At. Wt. of Ba = 0.137 Kg) by lighter Zn-ions (At. wt. of Zn = 0.065 Kg).

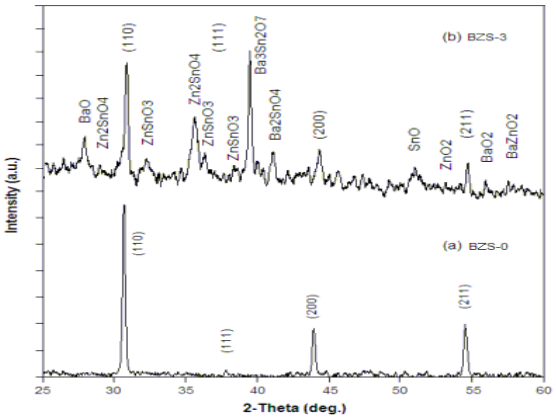

Fig. 2 X-ray diffraction pattern of the prepared $BaSnO_3$ (a) and $Ba_{0.5}Zn_{0.5}SnO_3$ (b) sintered at 1000 °C for 40 minutes.

Table 2 presents the structural parameters of the samples treated at 1000 °C for 40 minutes. One can see that the lattice parameter slightly decreases with increasing zinc concentration. Megrav [27] reported the lattice parameter for $BaSnO_3$ as a = b = c = 4.119 Å, which agrees well with the value obtained for our sample.

Table 2. Structural data for barium stannate sintered at 1000 °C for 40 minutes.

Sample symbol	Lattice constant (nm)	X-ray density d_x (g/cm^3)	Porosity p %	Bulk density d (g/cm^3)	Effective porosity p_{ef} (%)	Average grain size D_m (μm)	Specific surface area A_{sp} (m^2/g)
BZS0	0.41176	7.229	65.05	2.526	10.105	1.15	2.06
BZS1	0.40914	7.195	64.44	2.558	14.828	1.13	2.08
BZS2	0.40877	7.040	64.12	2.526	21.658	0.34	6.98
BZS3	0.40875	6.516	61.02	2.540	21.619	0.32	7.38

The porosity *p* of all the samples is high, between 61% and 65% due to the preparation method (by solid-state reaction technique, instead of chemical route method).

The effective porosity p_{ef} is diminished at the sample without zinc substitutions (10.1%) and higher in the case of the zinc substitutions (14.8% - 21.6%).

The SEM micrographs (Fig. 3 a, b and c) on the fracture surfaces of the samples revealed that the microstructure is affected by the amount of Zn^{2+} ions that substitute the Ba^{2+} ions in the barium stannate ($BaSnO_3$). Generally, all the samples are characterized by a fine granulation. The average grain sizes ranges between 0.32 μm (Fig. 3c) and ~1.1 μm (Fig. 3a). The barium stannate particles being small, a tendency towards agglomerations can be observed. One can also remark the change of the grain shape from faceted to rounded crystallites and pore coarsening when increasing the Zn^{2+} ions concentration. Large pores, above 1 μm in diameter, distributed along the grain agglomerations can be observed. In the case when these materials are used to produce humidity or gas sensors, pores are necessary for rapid sensor response, because the water or gas adsorption rate is controlled by the diffusion rate of water vapors or gas. These structures indicate that the investigated barium stannates can easily exhibit adsorption and condensation of water vapors.

Furthermore, the porous structure is an advantage in discouraging fracture due to thermal shock.

In Table 2 one can see that the Zn^{2+} ion concentration strongly influences the structural parameters. The average grain size of the specimens decreases and the specific surface area increases with increasing concentration of Zn ions. The largest specific surface area of 6.98 m^2/g and 7.38 m^2/g were found for the BZS-2 respectively BZS-3 samples, with the average grain size of about 300 nm and porosity of 21.6 % (Fig. 3c).

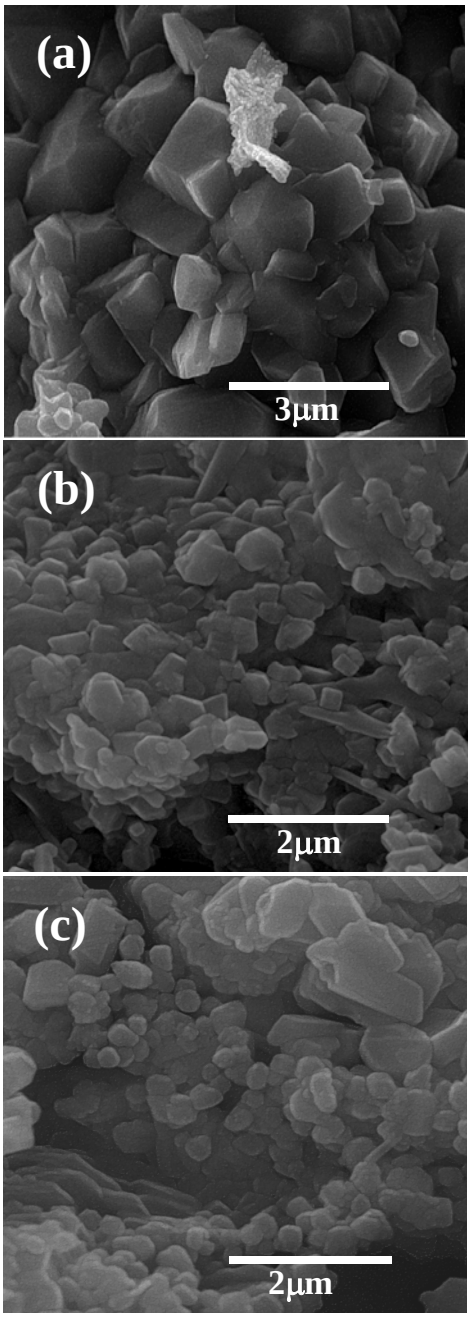

Fig. 3 SEM micrographs of $Ba_{0.9}Zn_{0.1}SnO_3$ (a), $Ba_{0.8}Zn_{0.2}SnO_3$ (b) and $Ba_{0.5}Zn_{0.5}SnO_3$ (c) samples.

In the oxide porous compounds, such as the barium stannate in our case, the gas molecules or water vapor will react not only with the grains from the material surface, but also with the material grains from inside the sensor element. At the same time, a larger specific surface belike implies a larger active surface exposed to the gas, as well as a higher sensitivity to gases and water vapor. The small area of the specific surface of the pure barium (BZS-0) can be the result of the higher concentration of the closed pores to the detriment of the open pores.

The observed modifications in the particle size and the area of specific surface suggest that the partial incorporation of the Zn^{2+} ions in the stannate crystals, and in consequence, the apparition of the secondary phases, inhibit the crystal increase and favor the increase of the specific surface area.

The substitution with x =0.2-0.5 results in radical microstructure changes (Fig. 3 b and c), consisting in the following:

- A significant diminution of the crystallites size, from about 1μ to about 300 nm;
- The formation of grain chains around large pores and of inter-connected pores in shape of capillary tubes between the grains chains;
- Absence of the grain agglomerations. It is possible that the presence of the foreign phases inhibits the growth and agglomeration process.

4. Conclusions

The most important conclusions are as follows:

Zinc-doped barium stannate having the general formula $Ba_{1-x}Zn_xSnO_3$, where x=0-0.5 were prepared by combustion method.

By the substitution of the Zn^{2+} ions in the barium stannate up x = 0.1, an increase of the effective porosity is obtained, while the crystalline structure remain relatively the same.

The lattice parameters for a high doping level, like in the case of the samples with x=0.2 and x=0.5, have very close values, which suggests the formation of secondary phases with zinc excess, and the determined values of the lattice parameters belong to the crystalline core that contains a smaller amount of zinc.

By increasing the substitution degree up to x = 0.5, the samples porosity remain at a high level; the crystal size quickly diminishes and the specific surface area increases.

The barium stannates with zinc substitutes with x = 0.2-0.5 prepared through the combustion method and treated in air for 40 minutes at 1000 ^oC, present a marked effective porosity, which remains constant on this entire doping interval, having the value of about 21.6%, specific surface area of ~7 m^2/g and an average grain size almost constant around the value of 300 nm.

Acknowledgement

The autors would like to acknowledge the financial support of POSDRU/89/1.5/S/49944.

References

[1] J. Cerda, J. Arbiol, R. Diaz, D. Dezanneau, J.R. Morie, Mater. Lett. **56**, 131 (2002).
[2] Y. Shimizu, Y. Fukuyama, T. Nrikio, H. Arai, T. Seiyama, Chem Lett. **3**, 377 (1985)**.**
[3] B. Ostrick, M. Fleischer, U. Lampe, H. Meixner, Sensors and Actuators B **44**, 601 (1997).
[4] M. Licheron, G. Jouan, E. Husson, J. Eur. Ceram. Soc. **17**, 1453 (1997).
[5] T. R. N. Kutty and R. Vivekanandan, Mater. Res. Bull. **22**, 1457 (1987).
[6] C. P. Udawatte, M. Kakihana, M. Yoshimura, Solid State Ionics, **108**, 23 (1998).
[7] S. Y. Jung, K. Seungwan, J. Ind. Eng. Chem. **7,** 183 (2001).
[8] S. Upadhyay, O. Parkash, D. Kumar, Journal of Alloys and Compounds **432**, 258 (2007).
[9] S. Upadhyay, P. Kavitha, Materials Letters **61**, 1912 (2007).
[10] B. Li, P. T. Lai, S. H. Zeng, M. Q. Huang, Smart Materials and Structures **9**, 498 (2000).
[11] S. Upadhyay, O. Parkash, D. Kumar, J. Electroceram. **18**, 45 (2007).
[12] A. M. Azad, M. Hashim, S. Bapist, A. Badri, A.U. Haq, J. Mater Sci. **35**, 5475 (2000).
[13] S. Upadhyay, O. Parkash, D. Kumar, J. Mater. Sci. Lett. **16**, 1330 (1997).
[14] A. M. Azad, L.L.W.Shyna, T.Y.Pang, C.H. Nee, Ceram. Int. **26**, 685 (2000).
[15] C. P. Udawatte, M. Kakihana, M. Yoshimura, Solid State Ionics, **108**, 23 (1998).
[16] S. Upadhyay, O. Parkash, D. Kumar, Materials Letters, **49**, 251 (2001).
[17] E. Rezlescu, C. Doroftei, P. D. Popa, N. Rezlescu, Journal of Magnetism and Magnetic Materials **320**, 796 (2008).
[18] P. D. Popa and N. Rezlescu, Romanian Reports in Physics, **52**, 769 (2000).
[19] C. Doroftei, P. D. Popa, N. Rezlescu, J. Optoelectron. Adv. Mater. **12**, 881 (2010).
[20] N. Rezlescu, C. Doroftei, E. Rezlescu, P. D. Popa, Sensors and Actuators B **115**, 589 (2006).
[21] S. Seto, S. Yamada, K. Suzuki, Solar Energy Materials & Solar Cells, **67,** 167 (2001).
[22] N. Rezlescu, C. Doroftei, E. Rezlescu, P. D. Popa, Phys. Stat. Sol. **A 203**, 306 (2006).
[23] S. Seto, S. Yamada, K. Suzuki, Solar Energy Materials & Solar Cells, **67**, 167 (2001).
[24] C. Laberty, P. Alphonese, J. J. Demai, C. Sarada, A. Rousset, Materials Research Bulletin **32**, 249 (1997).
[25] D. J. Kim, J. Amer. Ceram. Soc. **72**, 1415 (1989).
[26] J. Smith, A. J. E. Welch, Acta Crystallographica **13**, 653 (1960).
[27] H. D. Megraw, Proc. Phys. Soc.,Lond. **58**, 133 (1946).

*Corresponding author: docorneliu@yahoo.com